Nanoscale Res Lett (2008) 3:105–108
DOI 10.1007/s11671-008-9120-x

NANO EXPRESS

Size-dependent Fano Interaction in the Laser-etched Silicon Nanostructures

Rajesh Kumar · A. K. Shukla · H. S. Mavi · V. D. Vankar

Received: 13 November 2007 / Accepted: 14 February 2008 / Published online: 4 March 2008

Abstract Photo-excitation and size-dependent Raman scattering studies on the silicon (Si) nanostructures (NSs) prepared by laser-induced etching are presented here. Asymmetric and red-shifted Raman line-shapes are observed due to photo-excited Fano interaction in the quantum confined nanoparticles. The Fano interaction is observed between photo-excited electronic transitions and discrete phonons in Si NSs. Photo-excited Fano studies on different Si NSs show that the Fano interaction is high for smaller size of Si NSs. Higher Fano interaction for smaller Si NSs is attributed to the enhanced interference between photo-excited electronic Raman scattering and phonon Raman scattering.

Keywords Fano interference · Silicon nanostructures · Raman spectra

Introduction

Raman scattering from the silicon (Si) nanostructures (NSs) has been extensively studied in recent years [1–4]. Observed Raman line-shapes from the Si NSs are asymmetrically broadened and red-shifted from its counterpart for the bulk Si. Most authors have fitted the first-order experimental Raman band to an asymmetrical line-shape first proposed by Richter et al. [5] and then modified by Campbell et al. [6]. In this model, the asymmetry and red-shift in the Raman peak have been attributed to the confinement of phonons in the Si NSs. Many others [3, 4] have explained the asymmetry and downshift in the Raman line-shape in terms of a combined effect of quantum confinement and laser heating. Magidson and Beserman [7] have observed the Fano interference [8, 9] between photo-excited electrons and discrete phonons in bulk Si when Raman spectra were recorded using laser power density of 10^6 W/cm^2. However, the presence of photo-excited Fano interaction in Si NSs was proposed very recently where detailed photo-excitation-dependent Raman studies were carried out on the Si NSs [10]. An increase in the asymmetry ratio of Raman line-shape was noticed as a result of increasing excitation laser power density in the range 0.22–1.76 kW/cm^2. Effect of the quantum confinement on Fano resonance is not studied yet and needs further studies to elucidate the behavior of Fano interaction as a function of Si NSs size and laser power density.

The purpose of this paper is to study the Fano interaction in the Si NSs as a function of the NSs size and laser power density. The Si NSs of two different sizes are fabricated by laser-induced etching (LIE) method [11] by etching using two different etching times for same laser power. Surface morphology is studied by atomic force microscopy (AFM) to see the formation of quantum confined Si NSs. Raman spectra are recorded using two different laser power densities of 0.2 and 0.88 kW/cm^2 for both the samples. Raman spectra recorded using 0.2 kW/cm^2 are fitted using phenomenological phonon confinement model [5, 6] to calculate the most probable Si NSs size. Using these NSs sizes, Raman spectra recorded using 0.88 kW/cm^2 are fitted using Fano-Raman line-shape [10] to find the Fano asymmetry parameter to see the effect of Si NSs size on the Fano interaction. Higher Fano interaction is seen for smaller Si NSs as compared to large Si NSs.

R. Kumar · A. K. Shukla (✉) · H. S. Mavi · V. D. Vankar
Department of Physics, Indian Institute of Technology, Hauz Khas, New Delhi 110016, India
e-mail: akshukla@physics.iitd.ernet.in

Experimental Details

Two samples (samples A and B) containing Si NSs are fabricated by the LIE method [11]. The LIE is done by immersing a Si wafer (resistivity of 3–5 Ω cm) into 48% HF acid and then focusing a 500 mW argon-ion laser beam ($E_{ex} = 2.41$ eV) to a circular spot of 120-μm on the wafer. The etching time is 45 min for the sample A and 60 min for the sample B keeping other parameters (like laser power density, wavelength, and concentration of HF) the same. Raman scattering was excited using photon energy ~2.54 eV of the argon-ion laser at two different laser power densities of 0.2 and 0.88 kW/cm^2. The reason for choosing low laser power density is to avoid heating of the sample during Raman recording. Raman spectra were recorded by employing an SPEX-1403 doublemonochromator with HAMAMATSU (R943-2) photomultiplier tube arrangement and an argon ion laser (COHERENT, INNOVA 90).

Results and Discussions

Figure 1a, b shows AFM images of Si NSs formed in the samples A and B, respectively. The images shown in Fig. 1 are high-resolution images taken from the pore walls of the laser-etched samples. Figure 1a shows the formation of Si NSs having sizes in the range of a few nanometers. The Si NSs of smaller size are formed in the sample B in Fig. 1b due to increased etching time. Higher quantum confinement is expected in sample B as compared to sample A. The possibility of quantum confinement effect in these Si NSs is investigated by Raman experiments. Figure 2a shows Raman spectrum from the sample A recorded using an excitation laser power density of 0.2 kW/cm^2. Raman active optical phonon mode, which is observed at 520.5 cm^{-1} for the bulk Si, shifts toward lower wavenumber (518.5 m^{-1}) in Fig. 2a. The Raman line-shape has asymmetry ratio of 2.8 with FWHM of 12.5 cm^{-1} in Fig. 2a. Asymmetry and broadening in Raman line-shape is attributed to the quantum confinement of phonons in Si NSs [12–15]. The asymmetry ratio is defined here as Γ_l/Γ_h, where, Γ_l and Γ_h are half widths on the low- and high-energy side, respectively, of the maximum. Figure 2b displays Raman spectrum from the sample A when recorded using the excitation laser power density of 0.88 kW/cm^2. This Raman spectrum has peak at 518 cm^{-1} with asymmetry ratio of 3.1 and FWHM of 14 cm^{-1} in Fig. 2b. Figure 2b shows that asymmetry, red shift, and FWHM in Raman line-shape increase by the increasing excitation laser power density. Changes in the Raman line-shape are reversible in nature on decreasing the laser power density. This reveals that the asymmetry in Raman line-shape in Fig. 2b is not an effect of quantum confinement alone. Heating effect is ruled out because the laser power density is not high enough to do appreciable heating. Increase in the asymmetry on increasing excitation laser power density is due to Fano interaction between electronic Raman scattering involving photo-excited electrons within electronic states and usual optical phonon Raman scattering [10]. At higher laser power density of 0.88 kW/cm^2, the electronic Raman contribution increases because of more number of photo-excited electronic transitions. There is no effect of increased laser power density on phonon Raman scattering because of absence of the heating effect. These two effects combine to show high asymmetry ratio in Fig. 2b as compared to Fig. 2a.

Laser power density-dependent Raman spectra from smaller Si NSs in sample B are shown in Fig. 2c, d. Figure 2c, d is the Raman spectra from sample B when recorded using excitation laser power densities of 0.2 and 0.88 kW/cm^2, respectively. Raman spectrum in Fig. 2c has peak at 518 cm^{-1} with asymmetry ratio of 2.9 and FWHM

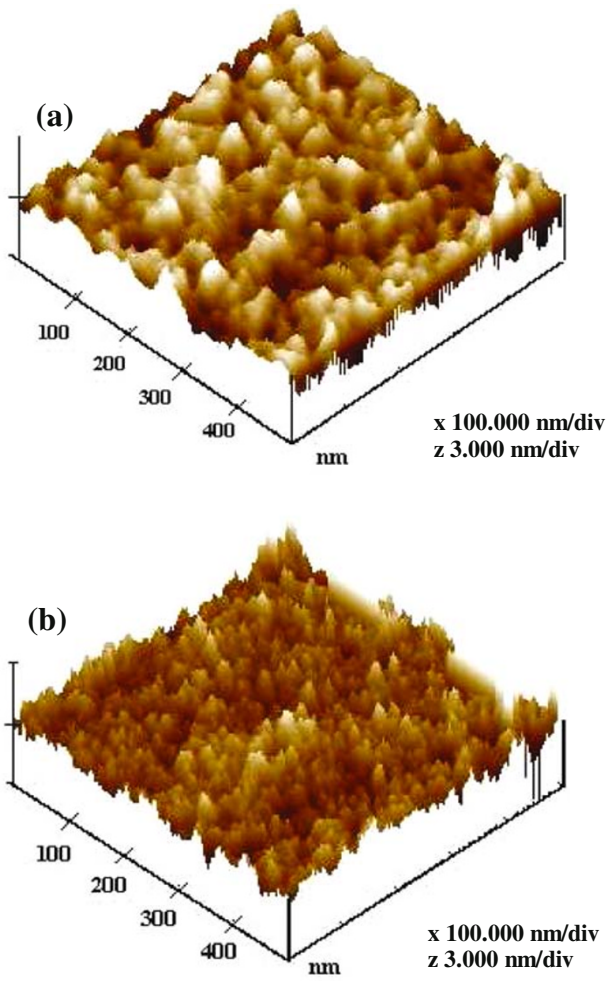

Fig. 1 AFM images showing silicon NSs in (**a**) the sample A and (**b**) the sample B

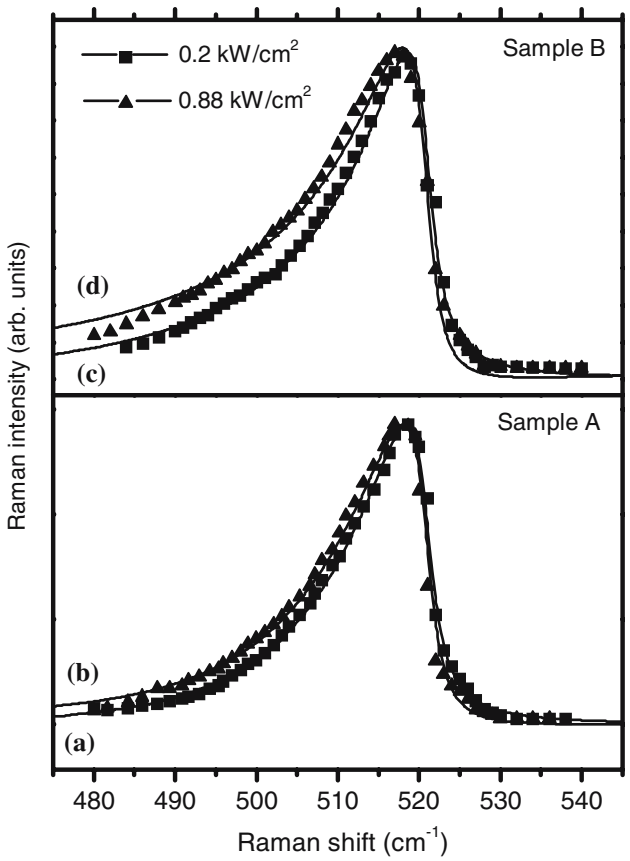

Fig. 2 Raman spectra from samples A and B. The calculated Raman spectra are indicated by solid line curves and the experimental data are plotted as discrete points. Phonon confinement model has been used to fit the experimental data in (**a**) and (**c**) whereas Eq. 1 is used to fit the data in the (**b**) and (**d**)

of 13.5 cm^{-1}. Higher asymmetry ratio and phonon softening in Fig. 2c as compared to Fig. 2a is due to higher quantum confinement effect from Si NSs in sample B than in sample A. The Raman spectrum peaked at 517 cm^{-1} with asymmetry ratio of 3.7 and FWHM of 16.5 cm^{-1} is observed in Fig. 2d due to photo-excited Fano interaction in sample B.

In order to quantitatively analyze the above-mentioned effects, the experimental data in the Fig. 2 are theoretically fitted with Fano line-shape for nanoparticles given by:

$$I(\omega) \propto \int_{L_1}^{L_2} N(L) \left[\int_0^1 \left\{ \frac{(\varepsilon + q)^2}{1 + \varepsilon^2} \right\} \cdot \exp\left(\frac{-k^2 L^2}{4a^2} \right) \cdot \mathrm{d}^2 k \right] \mathrm{d}L \tag{1}$$

where,

$$\varepsilon = \frac{\omega - \omega(k)}{\Gamma/2}.$$

The $\omega(k)$ is the phonon dispersion relation of the optic phonons of bulk Si given by

$$\omega(k) = \left(A + B \cos \frac{\pi k}{2} \right)^{1/2}$$

with $A = 171{,}400\ \mathrm{cm}^{-2}$ and $B = 100{,}000\ \mathrm{cm}^{-2}$. The '$q$' is Fano asymmetry parameter. The Γ, L, and 'a' are the line width, crystallite size, and lattice constant, respectively. The term in curly bracket takes care of the Fano interaction and the exponential term takes into account the confinement effect on Fano interaction in Si NSs of size 'L'. The '$N(L)$' is a Gaussian function of the form, $N(L) \propto [\exp -((L - L_0)/\sigma)^2]$, included to account for the size distribution of the nanocrystallites. The L_0, σ, L_1, and L_2 are the mean crystallite size, the standard deviation of the size distribution, the minimum, and the maximum confinement dimensions, respectively. Since Fano effect is negligible ($|1/q| \sim 0$) at low laser power density of 0.2 kW/cm^2 due to insufficient number of photo-excited electrons. Therefore, the experimental data in Fig. 2a, c shown as discrete squares are fitted by considering only phonon confinement effect (Eq. 1 of reference [11]). The theoretically obtained value of mean crystallite size (L_0) is 4.5 nm for sample A and is 3.0 nm for sample B. This implies that the quantum confinement effects are more pronounced in sample B than in sample A. All the fitting parameters used to fit the experimental Raman data in Fig. 2a, c are given in Table 1. It shows that distribution in Si NSs size is very narrow ($\sigma = 1$ nm) for both the samples. Qualitatively one can see that sizes from Raman results are in consonance with the AFM results in Fig. 1.

Experimental Raman data in Fig. 2b, d shown as discrete triangles are fitted with Fano-Raman line-shape of Eq. 1 with the appropriate L_0, L_1, and L_2 values obtained earlier for samples A and B as given in Table 1. In order to fit the experimental Raman data in Fig. 2b, d, 'q' is used as the fitting parameter. The experimental data in Fig. 2b, d show a good fitting for the Fano asymmetry parameter $|q|$ equal to 16 and 10 for the samples A and B, respectively. It reveals higher photo-excited Fano interaction in the smaller size NSs (sample B) as compared to larger size NSs (sample A). While fitting Raman data, the value of 'q' was kept constant for a given L_0, where the distribution of size is very narrow ($\sigma = 1$ nm). The smaller sizes present in the sample B are much smaller in size as compared to the Bohr's exciton radius of 5 nm for Si [16]. Thus, the confinement effect will be more in sample B in comparison

Table 1 Different fitting parameters used to fit the Raman line-shapes from samples A and sample B in the Fig. 2

Sample	L_0 (nm)	L_1 (nm)	L_2 (nm)	σ (nm)
Sample A	4.5	3.5	5	1
Sample B	3	2.5	4	1

with sample A. Quantum confinement of electrons lead to discrete energy levels. Photo-excited electrons interact with incident photon by electronic Raman scattering. This is possible when photo-excited electrons make transitions between discrete levels. Electronic Raman scattering may interfere with usual optical phonon scattering when optical phonon energy lies in the region $\Delta E = E_1 - E_2$ (where, E_1 and E_2 are energy of discrete electronic levels). Probability of interference increases in the smaller size NSs where discrete electronic levels are separated by optical phonon energy. Such type of Fano interaction cannot be seen in bulk Si or larger sized NSs. Fano interaction can be seen in the bulk Si when doping is above 10^{19} cm^{-3} [17]. Therefore, size-dependent Fano interaction in Si NSs is due to quantum confinement of electrons and phonons in laser-etched Si.

Conclusions

In summary, the Raman line-shapes from the Si NSs are investigated as a function of Si NSs size and excitation laser power density. The Raman line-shape becomes more asymmetric, wider, and shifts to lower wavenumber when the Raman spectra are recorded with higher laser power density. This behavior is attributed to the Fano interference between discrete phonons and photo-excited electronic transitions. Fano interaction is more pronounced for smaller size NSs at same laser power density. In other words, smaller size NSs will start showing photo-excited Fano interaction at lower excitation laser power density than for larger size NSs. Higher quantum confinement of photo-excited electrons and phonons in smaller Si NSs is responsible for observation of size-dependent photo-excited Fano interaction in laser-etched Si NSs.

Acknowledgments Authors acknowledge the financial support from the Department of Science and Technology, Goverment of India under the project "Optical studies of self-assembled quantum dots of semiconductors". One of the authors (R. Kumar) acknowledges the financial support from Council of Scientific and Industrial Research (CSIR), India. Technical support from Mr. N.C. Nautiyal is also acknowledged.

References

1. R. Wang, G. Zhou, Y. Liu, S. Pan, H. Zhang, D. Yu, Z. Zhang, Phys. Rev. B **61**, 16827 (2000)
2. S. Prusty, H.S. Mavi, A.K. Shukla, Phys. Rev. B **71**, 113313 (2005)
3. M.J. Konstantinovic, S. Bersier, X. Wang, M. Hayne, P. Lievens, R.E. Silverans, V.V. Moshchalkov, Phys. Rev. B **66**, 161311 (2002)
4. S. Piscanec, M. Cantoro, A.C. Ferrari, J.A. Zapien, Y. Lifshitz, S.T. Lee, S. Hofmann, J. Robertson, Phys. Rev. B **68**, 241312 (2003)
5. H. Richter, Z.P. Wang, L. Ley, Solid State Commun. **39**, 625 (1981)
6. I.H. Campbell, P.M. Fauchet, Solid State Commun. **58**, 739 (1986)
7. V. Magidson, R. Beserman, Phys. Rev. B **66**, 195206 (2002)
8. U. Fano, Phys. Rev. **124**, 1866 (1961)
9. M. Balkanski K.P. Jain R. Beserman M. Jouanne, Phys. Rev. B **12**, 4328 (1975)
10. R. Kumar, H.S. Mavi, A.K. Shukla, V.D. Vankar, J. Appl. Phys. **101**, 064315 (2007)
11. H.S. Mavi, S. Prusty, M. Kumar, R. Kumar, S. Rath, A.K. Shukla, Phys. Stat. Sol (a) **203**, 2444 (2006)
12. N. Fukata, T. Oshima, K. Murakami, T. Kizuka, T. Tsurui, S. Ito, Appl. Phys. Lett. **86**, 213112 (2005)
13. H.S. Mavi, A.K. Shukla, R. Kumar, S. Rath, B. Joshi, S.S. Islam, Semicond. Sci. Technol. **21**, 1627 (2006)
14. B. Pivac, K. Furic, D. Desnica, J. Appl. Phys. **86**, 4383 (1999)
15. B. Li, D. Yu, S. Zhang, Phys. Rev. B **59**, 1645 (1999)
16. A.G. Cullis, L.T. Canham, P.D.J. Calcott, J. Appl. Phys. **82**, 909 (1997)
17. N.H. Nickel, P. Lengsfeld, I. Sieber, Phys. Rev. B **61**, 15558 (2000)